Neurobiology of Disease 158 (2021) 105477

Contents lists available at ScienceDirect

Neurobiology of Disease

journal homepage: www.elsevier.com/locate/ynbdi

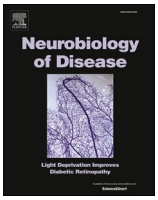

DNAJB6 suppresses alpha-synuclein induced pathology in an animal model of Parkinson's disease

Sertan Arkan [a], Mårten Ljungberg [a], Deniz Kirik [b], Christian Hansen [a,c,*]

[a] Lund University, Molecular Neurobiology, Department of Experimental Medical Science, BMC B11, 221 84 Lund, Sweden
[b] Brain Repair and Imaging in Neural Systems, Department of Experimental Medical Science, Lund University, BMC D11, Lund 22184, Sweden
[c] Department of Technology, University College Copenhagen, Denmark

ARTICLE INFO

Keywords:
Protein homeostasis
Parkinson's disease
Alpha-synuclein
Adeno associated virus
DNAJB6
Heat shock protein 70

ABSTRACT

Background: α-synuclein (α-syn) aggregation can lead to degeneration of dopaminergic neurons in the *substantia nigra pars compacta* (*SNpc*) as invariably observed in patients with Parkinson's Disease (PD). The co-chaperone DNAJB6 has previously been found to be expressed at higher levels in PD patients than in control subjects and was also found in Lewy bodies. Our previous experiments showed that knock out of DNAJB6 induced α-syn aggregation in cellular level. However, effects of overexpression of DNAJB6 against α-syn aggregation remains to be investigated.

Methods: We used a α-syn CFP/YFP HEK293 FRET cell line to investigate the effects of overexpression of DNAJB6 in cellular level. α-syn aggregation was induced by transfection α-syn preformed fibrils (PPF), then was measured FRET analysis. We proceeded to investigate if DNAJB6b can impair α-syn aggregation and toxicity in an animal model and used adeno associated vira (AAV6) designed to overexpress of human wt α-syn, GFP-DNAJB6 or GFP in rats. These vectors were injected into the SNpc of the rats, unilaterally. Rats injected with vira to express α-syn along with GFP in the SNpc where compared to rats expressing α-syn and GFP-DNAJB6. We evaluated motor functions, dopaminergic cell death, and axonal degeneration in striatum.

Results: We show that DNAJB6 prevent α-syn aggregation induced by α-syn PFF's, in a cell culture model. In addition, we observed α-syn overexpression caused dopaminergic cell death and that this was strongly reduced by co-expression of DNAJB6b. The lesion caused by α-syn overexpression resulted in behavior deficits, which increased over time as seen in stepping test, which was rescued by co-expression of DNAJB6b.

Conclusion: We here demonstrate for the first time that DNAJB6 is a strong suppressor of α-syn aggregation in cells and in animals and that this results in a suppression of dopaminergic cell death and PD related motor deficits in an animal model of PD.

1. Background

Parkinson's disease (PD) is the most common neurodegenerative movement disorder. It is primarily caused by a selective loss of dopaminergic neurons in the *substantia nigra pars compacta* (*SNpc*) (Goedert et al., 2013; Hansen and Li, 2012; Vekrellis et al., 2011; Waxman and Giasson, 2009). This neurodegenerative process correlates with the formation of large protein-rich cytoplasmic inclusions, known as Lewy bodies (LBs), in which aggregated α-syn is main protein component (Hansen and Li, 2012; Vekrellis et al., 2011; Waxman and Giasson, 2009; Spillantini et al., 1997). The *SNCA* gene, which encodes α-syn, is also linked to familial forms of PD, caused by missense mutations, which

Abbreviations: AAV, Adeno associated virus; AB42, Amyloid beta-42; α-syn, alpha synuclein; ALS, Autophagy-lysosome pathway; AP, Anteroposterior; CFP, Cyan fluorescence protein; DMEM, Dulbecco's modified eagle's medium with GlutaMAX-I; DV, Dorsoventral; EDTA, Ethylenediaminetetraacetic acid; FBS, Fetal Bovine Serum; FRET, Förster resonance energy transfer; GFP, Green fluorescence protein; HD, Hungtington disease; HSP70, Heat shock protein 70; IHC, Immunohistochemistry; LB, Lewy body; ML, Mediolateral; PBS, Phosphate Buffered Saline; PBS-T, Phosphate Buffered Saline with Tween 80; PD, Parkinson's disease; PPF, Preformed fibril; polyQ74, polyQ74exon1huntingtin; P/S, penicillin/streptomycin; PVDF, Polyvinylidene fluorid; RT, Room temperature; SDS PAGE, Sodium dodecyl sulphate-polyacrylamide gel electrophoresis; SN, Substansia nigra; SNpc, Substansia nigra pars compacta; TBS, Tris buffered saline; TBS-T, Tris buffered saline with Triton X-100; TH, Tyrosine hydroxylase; UPS, Ubiquitin-proteasome system; YFP, Yellow fluorescence protein.

* Corresponding author at: Department of Technology, University College Copenhagen, Denmark
E-mail addresses: sertan.arkan@med.lu.se (S. Arkan), deniz.kirik@med.lu.se (D. Kirik), christian.hansen@med.lu.se, crha@kp.dk (C. Hansen).

https://doi.org/10.1016/j.nbd.2021.105477
Received 17 February 2021; Received in revised form 5 July 2021; Accepted 9 August 2021
Available online 11 August 2021

result in increased aggregation of the protein. It is therefore believed that α-syn aggregation plays a key role in PD pathogenesis. α-syn is abundantly expressed in neurons and plays a role in exocytosis (Bonini and Giasson, 2005; Burre et al., 2010; Logan et al., 2017). α-syn does not normally form large aggregates in neurons, despite that it is highly expressed, because of an effective protein homeostasis system (Auluck et al., 2002; Balch et al., 2008; Cuervo et al., 2004; Hartl et al., 2011). 70 kDa heat shock protein (Hsp70) plays a major protective role against protein aggregation and can prevent aggregation of α-syn (Auluck et al., 2002; Aprile et al., 2015; Gao et al., 2015; McLean et al., 2004). However, a large body of work has shown that Hsp70 does not directly recruit protein substrates *in vivo*, but do so with help from co-chaperones, such as the DNAJ proteins (De Mattos et al., 2020; Qiu et al., 2006). DNAJB6, is expressed in neurons, and has been found to be present in LBs of PD patients (Durrenberger et al., 2009). We have previously identified that DNAJB6 is a suppressor of α-syn aggregation in a cell line model and in *in vitro* based studies, in a HSP70 dependent manner (Aprile et al., 2017). In support of this, we also found that DNAJB6 prevents α-syn aggregation induces by α-syn preformed fibrils (PFFs), using an unbiased α-syn FRET system to quantify α-syn aggregation (Deshayes et al., 2019). Other labs have shown that, DNAJB6b suppress aggregation of multiple amyloid proteins in cells (Gillis et al., 2013; Mansson et al., 2014a; Mansson et al., 2014b) and recently it is shown that DNAJB6b suppresses disease progression, in an HD mouse model (Kakkar et al., 2016). As we have so far only explored if DNAJB6 is a suppressor in non-neuronal cell line models and *in vitro*, we wanted to explore if DNAJB6 could prevent α-syn induced behavioral deficits and toxicity in an α-syn overexpression based animal model of PD. Here we show that DNAJB6b does indeed impair α-syn induced behavioral deficits by preventing α-syn induced death of dopaminergic neurons in the *SNpc*.

2. Materials and methods

2.1. Cell Culture, plasmids and transfections

HEK293 cells stably expressing α-*syn*-CFP α-syn-YFP were a kind gift from professor Marc Diamond and were generated as described in (Holmes et al., 2014). Cells were maintained in Dulbecco's Modified Eagle's Medium with GlutaMAX-I (DMEM) (Thermo Fisher Scientific, US), 10% heat inactivated fetal bovine serum (FBS) (Thermo Fisher Scientific, US) and 1% penicillin/streptomycin (P/S) (Thermo Fisher Scientific, US) and incubated at 37 °C, 5% CO_2 in humidified condition. Lipofectamine Ltx was used for transfection of mCherryDNAJB6 and mCherry plasmids according to manufacturer protocol (Thermo Fisher Scientific, US) 72 hours prior to FRET analysis and Lipofectamine 2000 was used to transfect preformed α-synuclein fibrils at 10 nM final concentration 48 hours prior to FRET analysis. Preformed fibrils synthesis and transfection were performed as described in (Deshayes et al., 2019). mCherry expression plasmid was generated by replacing mCherry with AcGFP in the pAcGFP-C1 vector using restriction enzymes and the mCherry-DNAJB6 was subsequently generated by amplifying human DNAJB6b cDNA using primers 5'gtcactcgagctatggtggattactatgaagttctaggcgtg3' and 5′ gtcaggatccttacttgttatccaagcgcagcagctg3' which contained restriction enzyme overhangs, followed by insertion of the cDNA into the pmCherry-C1 vector using the restriction enzymes *Xho*I and BamHI.

2.2. Florescence Resonance Energy Transfer (FRET)

FRET experiments were performed on a BD LSR Fortessa with the software BD FACS Diva 8.0.1 (BD Biosciences,US). Gates for analysis were calibrated using single stained controls as well as negative controls. YFP was excited using a 488 nm laser and emitted light was detected using a 530/30 nm bandpass filter. CFP was excited at 405 nm and the emitted light was detected using a 442/46 nm bandpass filter. mCherry was excited at 488 nm and the emitted light was detected using 610/20 nm bandpass filter. FRET was measured by excitation of CFP using a 405 nm laser and the fluorescence was captured using 525/50 nm bandpass filter.

2.3. Western blot

The cells were washed with phosphate buffered saline (PBS) and subsequently lysed in a lysis buffer (0.5% Triton X-100, 50 mM Tris HCl, 175 mM NaCl and 5 mM Ethylenediaminetetraacetic acid (EDTA), pH 8, 1:100 protease inhibitor cocktail (Sigma-Aldrich, US) on ice for at least 15 minute (min). The cell debris was spun down at 15,000 rcf for 10 min at 4C, and the supernatant was collected. Cell lysates mixed with 25% 4X Laemmli buffer containing 10% of 0.1 M Dithiothreitol (DTT), and boiled for 5 min at 96 °C. 25 μg of proteins from lysate samples were separated on 10% SDS-PAGE polyacrylamide gels, then the samples transferred into Polyvinylidene fluorid (PVDF) membranes using the Trans-Blot Turbo Transfer System (Bio-Rad, US). The membrane was blocked with 5% skimmed milk powder (Sigma Aldrich, US) dissolved in PBS containing 0.05% Tween (PBS-T) for 1 hour at room temperature (RT), after which they were washed thrice for 5 min with PBS-T at RT. Subsequently, the membrane incubated in 2% skimmed milk in PBS-T with 1:2000 anti-DNAJB6 primary antibody (Proteintech, US) overnight shaking at 4 °C. The next day, the membrane was washed thrice in PBS-T for 5 min and then incubated shaking at RT for 1 h in 3% skimmed milk in PBS-T with 1:5000 anti-rabbit secondary antibody (Dako, Denmark). The membrane was washed then thrice for 5 min in PBS-T. Western Blotting Luminol Reagent (Santa Cruz Biotechnology,US) was used for chemiluminescence reactions and protein bands were developed using a ChemiDoc™ XRS+ Molecular Imager (Bio-Rad, US) and the Image Lab software (Bio-Rad,US). After stripping the membrane for 15 min at RT (Restore Buffer, Thermo Fisher Scientific, US). The membrane was washed twice with PBS-T for 5 min and then blocked in 5% skimmed milk in PBS-T for 30 min before being incubated with a 1:10000 HRP coupled anti-β-actin primary antibody (Sigma Aldrich, US) and developed as described above.

2.4. Animal housing

Female Sprague–Dawley rats (imported at a weight of 225 to 250 g; Charles River Germany) were housed with *ad libitum* access to food and water under a 12-h light/dark cycle.

2.5. Experimental design

The rats were unilaterally injected with either cocktails of AAV6-human wild type (wt) α-syn and AAV6-GFP or AAV6- human wt type α-syn and AAV6 DNAJB6-GFP vectors into the *SNpc*. Cylinder and stepping tests performed just before stereotaxic injection (to create a baseline control) and after 4 weeks, 8 weeks and 12 weeks, to evaluate the motor functions of the rats. After completing the behavioral tests, the rats were euthanized and immunohistochemical (IHC) staining were performed.

2.6. rAAV vector production

An AAV6 vector expressing human wild-type α-syn under the human synapsin-1 promoter was used in this study as described (Landeck et al., 2016; Ulusoy et al., 2012). The vector titer of α-syn and GFP mixture was 4.4×10^{13} human wt α-syn and GFP-DNAJB6 vector mixture was 4.4×10^{13} genome copies/mL. AAV6 GFP- DNAJB6 vector was produced in Vigene Bioscience (US).

2.7. Stereotaxic injections

The rats were anesthetized by intraperitoneal injection of 6 mL/kg of

a 20:1 mixture of Fentanyl and Dormitor (Apoteksbolaget, Sweden). After placing the animal into a stereotaxic frame (Stoelting, Wood Dale, USA), 2 ul of rAAV6 vector cocktails were unilaterally injected into the substantia nigra (SN) using the following coordinates from: anteroposterior (AP) -5.0 mm, mediolateral (ML) -2.0 mm from bregma and dorsoventral (DV) -7.2 mm from the dura. The tooth bar was adjusted to −2.3 mm. Injection was performed using a pulled glass capillary (Stoelting, Wood Dale, USA) fixed into a 5 uL Hamilton syringe with a blunt 22 s gauge needle. The viral vectors injected at a constant rate (0.1 uL every 15 s), the glass capillary was held in place for 5 min, subsequently, retracted 0.1 mm and after 1 min it was slowly withdrawn from the brain. Temgesic and anti-sedan (Apoteksbolaget, Sweden) were administered subcutaneously as analgesic and to reverse anesthesia.

2.8. Behavioral tests

Behavioral tests were performed before stereotaxic injections as control, and after at 4 weeks, 8 weeks, and 12 weeks by the same researcher.

Stepping Test: Stepping test was performed to evaluate forelimb akinesia as described in (Kirik et al., 2000). Briefly, the number of steps counted by the left and right forepaws when passively moved along a 90 cm trajectory in forehand and backhand directions. The rats were trained to complete the test prior to experiments and the average of 3 trials were used in statistical analysis. The data are presented contralateral forehand forepaw contacts as percentage of right forehand forepaw contacts.

Cylinder Test: The cylinder test was used to evaluate the motor functions of rats as described in (Kirik et al., 2000). The rats were allowed to move freely in a clear glass cylinder. Mirrors were placed behind the cylinder to be able to observe all forelimb contacts on the glass wall. The videotapes were evaluated by an observer to the identity of the animals and the number of left and right paw touches on the cylinder wall were counted for 25 contacts. The data are presented contralateral (left) forepaw contacts as percentage of right paw contacts.

2.9. Immunohistochemistry

The rats were euthanized at 12 weeks after AAV injection by an overdose of sodium pentobarbital and perfused *via* the ascending aorta first with 50 mL/min of 0.9% NaCl for 1 min followed by 50 mL/min of ice-cold 4% paraformaldehyde (PFA in 0.1 M phosphate buffer, pH 7.4) for 5 min. Brains were removed and post-fixed in 4% PFA overnight and then transferred into 25% sucrose for cryoprotection at 4 °C for a minimum of 2 days. Subsequently, the brains were cut into 40 um thick 8 series of coronal sections on a microtome (Leica, Germany) and stored in an anti-freeze solution (0.5 M phosphate buffer, 30% glycerol, 30% ethylene glycol) at −20 °C. IHC staining of tyrosine hydroxylase (TH) were performed as free floating sections at RT. The sections were washed from anti-freeze solution using tris-buffered saline (TBS) buffer (5 mM Tris, 15 mM NaCl). The endogenous peroxidase activity in the sections were quenched by incubation in 3% H_2O_2 (Sigma Aldrich) and 10% methanol in TBS buffer for 30 min. After thrice washes with TBS buffer, sections were incubated in 0.05% Triton X-100 (Sigma Aldrich) in TBS buffer (TBS-T) containing 5% of rabbit normal serum (Vector Laboratories Inc., US) matching the species used to raise the secondary antibody for that protocol. This was performed for 1 h to eliminate non-specific secondary antibody binding. Anti- TH primary antibody (Abcam, cat# ab113) was diluted as 1:2000 in 1% BSA in TBS-T overnight at RT. The second day, the sections were thrice washed with TBS-T for 10 min and incubated with the biotinylated anti-sheep secondary antibody (1:200, Vector Laboratories Inc., US) in 1% BSA in TBS-T for 1 h. Sections were again washed with TBS-T for 10 min and incubated with an avidin-biotin-peroxidase complex solution (Vectastain ABC kit, Vector Laboratories Inc., US) for 1 h. The specific staining was visualized using 3,30-diaminobenzidine (Vectastain DAB Substrate kit, Vector Laboratories Inc., US) For preservation and visualization sections were mounted on chromatin-gelatin coated glass slides, dehydrated in increasing alcohol solutions, cleared in xylene and coverslipped using DPX (Sigma Aldrich).

2.10. Immunofluorescence stainings

Immunofluorescence staining was performed with anti-TH (Abcam, cat# ab113 (working dilution 1:2000)), mouse anti α-syn (BD bioscience, cat# 610787 (working dilution 1:1000)) and rabbit anti-p129 α-syn (Abcam, Cat#51253 (working dilution 1:1000)) antibodies. The free-floating sections were washed thrice with PBS from anti-freeze solution. The sections were then incubated in 0.025% Triton X-100 (Sigma Aldrich) in PBS containing 5% of normal serums (Vector Laboratories Inc., US) matching the species used to raise the secondary antibody for that proper staining for 1 h. Primary antibodies were diluted in PBS and overnight incubated at 4 °C. The next day, the sections were washed thrice with PBS for 5 min, then incubated with Cy3 and Cy5 (working dilution 1:300) fluorophore conjugated secondary antibodies (Jackson Immunoresearch, US). The sections were mounted on positive charged superfrost plus glass slides (ThermoScientific, US) and cover-slipped using PVA/DABCO. The immunofluorescence staining was visualized on a Leica SP8 laser-scanning confocal microscope (Leica, Germany).

2.11. Cell counting analysis

The experimental groups were randomized, and the assessment of TH (+) cell number and the quantification of phosphorylated α-syn aggregations were performed blindly. Light microscope (Zeiss Primostar, Germany) was used to visualize DAB stained neurons. Tyrosine hydroxylase positive (TH+) neurons were manually quantified in only a specific section that SN is separated from ventral tegmental area by medial terminal nucleus of accessory optic system (AP: −5.20 from Bregma). Data expressed as percent value of the contralateral side of the section. Fluorescence microscope was used to visualize neural cell bodies and the quantification of phosphorylated α-syn aggregations (Nikon Eclipse 80i). We counted number of triple stained cell bodies in the whole SNpc region. GFP represents AAV mediated gene expression, Cy3 filter represents phosphorylated α-syn aggregations, Cy5 filter represents to TH cell. All data presented means ± SEM.

2.12. Optical densitometry

Optical density of TH+ fibers was analyzed on digital images of coronal striatal sections obtained using a microscope (Nikon Eclipse 80i, Japan). For each animal the optical density was measured at seven rostocaudal levels over the whole striatum according to the rat brain atlas Paxinos and Watson (2006) AP, +1.6; AP, +1.0; AP, +0.2; AP, −0.3; AP, −0.9; AP, −1.4; and AP, −2.1 relative to bregma. – was outlined using IMAGEJ software (version 1.50i, NIH, USA). Optical density readings were corrected for non-specific background using density measurements from the corpus callosum of each animal. Data presented are means ± SEM from all brains and expressed as percent of contralateral side values.

2.13. Statistical analysis

All behavioral data were analyzed by repeated measure two-way ANOVA followed by *post hoc* Bonferroni test. Counting of TH positive neurons in the *SNpc*, quantification of the optical fiber density in the striatum, the quantification of phosphorylated α-syn aggregations and quantitative FRET measurements of cell culture experiments were analyzed by independent *t*-test (Graphpad Prism 6, US), assuming normal distribution. $P < 0.05$ were considered statistically significant. All data are expressed as means ± SEM.

3. Results

3.1. Overexpression of DNAJB6 is protect against α-syn aggregation in cellular model of PD

We have previously shown that α-syn PFF seeded α-syn aggregation was increased in a HEK293 cell line, stably expressing α-*syn*-CFP and α-syn-YFP (hereafter named α-syn FRET cells), when DNAJB6 was knocked out (Deshayes et al., 2019). Here, we examined if overexpression of DNAJB6 would suppress α-syn aggregation induced by PFF's in the same cell line set up, and observed that overexpression of DNAJB6 decreased the seeded α-syn aggregation more than 4-fold (Fig. 1A and B). This observation showed that increasing DNAJB6 expression in cells protects against α-syn aggregation.

3.2. AAV6 mediated overexpression of DNAJB6 rescue to cell death in SN

Next, we wanted to investigate if the protective effect of DNAJB6 against α-syn aggregation seen in cells, could also protect against toxic α-syn aggregation in an α-syn overexpression based animal model of PD. We therefore set up a rat model, in which we induced α-syn overexpression in the *SNpc* by use of viral vectors incorporated into AAV6 vira. Two groups of 9 rats each were unilaterally injected with either AAV6/ human wt α-syn and AAV/GFP (control) or AAV6/ human wt α-syn and AAV/GFP-DNAJB6 vectors. Of these rats were 8 of 9 from each group showed successful targeting the *SNpc*, as shown in representative images (Fig. 2A-H). Rats co-injected with vector expressing α-syn and GFP displayed far less TH positive neurons in injected *SNpc* compared to non-injected control side (%33.62 ± 7.404, n:8), whereas rats injected with vectors to induce expression of human wt α-syn and GFP-DNAJB6, showed substantially more TH positive cells in the injected side (%61.34 ± 8.162, n:8), suggesting that DNAJB6 protects against α-syn induced neuronal cell death (df:14, t:2.515, p:0.0247) (Fig. 2K and L). While there was a clear difference in cell loss of the dopaminergic neurons in the *SNpc* between the groups, TH staining of the striata revealed that there was some loss of TH + optical fiber density in both groups of rats on injected side compared to contralateral control striata, but also that the TH density loss was similar (df:14, t:0.06363, p:9502) in both human wt α-syn and GFP (%62.74 ± 10.17,n:8) and human wt α-syn and GFP-DNAJB6 groups (%61.99 ± 5.951, n:8) (Fig. 3A - E).

3.3. Overexpression of DNAJB6 attenuate motor impairments

To evaluate the gradual locomotor impairment caused by α-syn overexpression and the potential protective effect of DNAJB6 expression, we performed stepping and cylinder tests on the animals before injection and at 4, 8 and 12 weeks post-injection. The group expressing α-syn and GFP in the *SNpc* showed gradually deterioration in stepping tests from 4 to 12 weeks. In comparison, the overexpression of DNAJB6 rescued to the motor behavior impairments of rats in stepping test. Fig. 4A (F :12.96, $p < 0.0001$) and Fig. 4B (F :6.658, p: 0,0009). We were not able to find any significant difference between groups in a complementary cylinder test (Fig. 4C (F:0.5468, p:0,6530)). However, it is also well known that in order to see behavioral differences in cylinder test, it does require a higher extend of dopaminergic cell deathin order to see behavioral difference in stepping test. Therefore, these results fit in line with this fact.

3.4. Overexpression of DNAJB6 might cause to changes in phosphorylated α-syn (at serine129) in SN

α-syn toxicity is linked to its ability to form aggregates and it has been shown that aggregated α-syn is more phosphorylated at S129 (Fujiwara et al., 2002). Therefore, we stained the brain sections containing *SNpc* with anti-TH and anti-pS129-syn antibodies (Supplementary Fig. 1). Although we did not find any statistically significant difference between our groups, we had interesting trend in our results. We observed that the group that expressed α-syn and GFP in *SNpc* showed less tendency to p129-syn staining in the TH positive cells, compare to the group that expressed α-syn and GFP-DNAJB6 ($t = 1.535$, df = 14, $p = 0.147$). This situation could be based on the number of surviving TH (+) cells in α-syn and GFP-DNAJB6 group were more than in α-syn and GFP group. Therefore, we observed there is a strong tendency more phosphorylated α-syn at S129 in α-syn + GFP-DNAJB6 group than α-syn + GFP group (Supplementary Fig. 2A). We also counted number of GFP + cells, which express phosphorylated α-syn at S129, for both groups. We did not observe overall difference between our groups ($t = 0.6161$, df = 14, $p = 0.5477$) (Supplementary Fig. 2B).

4. Discussion

Here we demonstrate for the first time that expression of a DNAJ protein can impair disease pathology in an animal model of PD. Increased aggregation of α-syn is linked to PD pathology (Venda et al.,

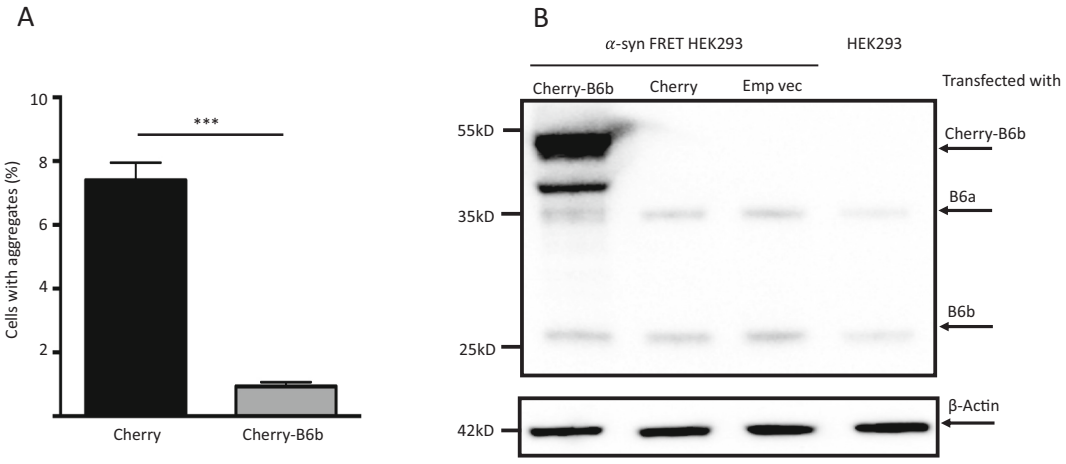

Fig. 1. Overexpression of DNAJB6 leads to suppression of α-syn in α-*syn*-CFP, α-syn-YFP HEK293 cell line. (A) Percentage of cells displaying FRET signal, expressing DNAJB6-mCherry or mCherry (control), 72 h subsequent to plasmid transfection and 48 h subsequent to inducing α-syn aggregation with 10 nM α-syn PFF's ($n = 3$). (B) Western blot displaying expression of DNAJB6b in lysates from α-syn FRET HEK293 cells transfected with DNAJB6b or mCherry transfected control cells. Membrane was probed with anti-DNAJB6 and anti-β actin antibodies. All data are presented as mean ± SEM. ***$P < 0.001$. Data was analyzed by unpaired *t*-test.

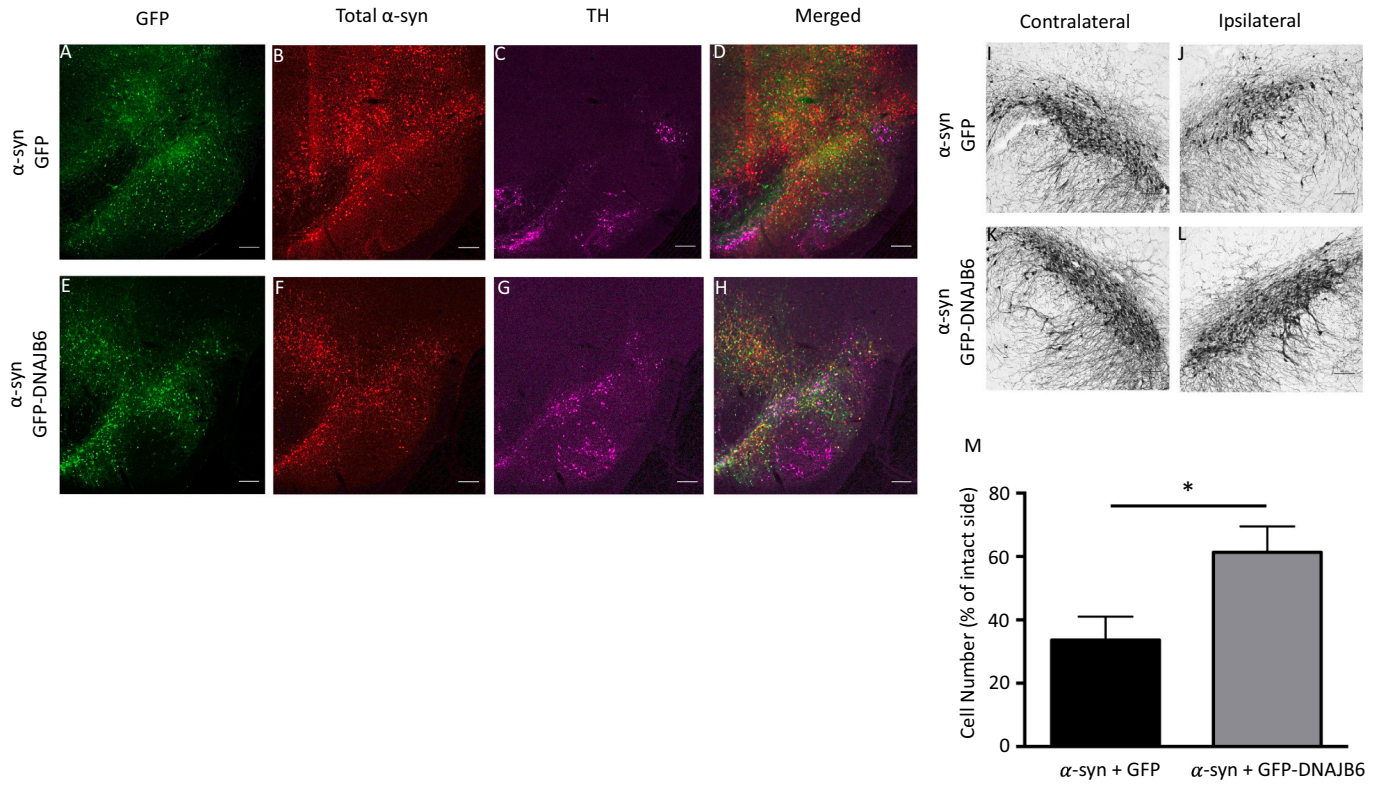

Fig. 2. DNAJB6 expression protects against α-syn induced loss of dopaminergic neurons in the *SNpc*. Representative pictures of *SNpc* stainings with anti-TH (purple) and anti-α-syn (red) combined with GFP fluorescence (green) in 40 μm brain tissue sections from rats injected with either AAV6/ human wt α-syn and AAV6/GFP vectors (A-D) or AAV6/ human wt α-syn and AAV6/GFP-DNAJB6 vectors (*E*-H). Representative images of *SNpc* from rats injected with AAV6/ human wt α-syn and AAV6/GFP stained with anti-TH antibody, depicting the contralateral (I) and the ipsilateral (J) *SNpc* of the injected rats, with the ipsilateral side displaying less TH+ neurons (%33.62 ± 7.404, $n = 8$) (J). Representative images of *SNpc* from rats injected with AAV6/α-syn and AAV6/GFP-DNAJB6 stained with with anti-TH antibody, depicting the contralateral (K) and the ipsilateral (L) *SNpc* of the injected rats, with the ipsilateral side displaying less TH+ neurons (%61.34 ± 8.162, n = 8). (M) Quantification of TH+ cell number in the *SNpc*, which are expressed as a percentage of the contralateral side ($P < 0.05$) analyzed by unpaired t-test (df = 14, $t = 2.515$, $p = 0.0247$). All data are presented as mean ± SEM. Scale bars, 100 μm. (For interpretation of the references to colour in this figure legend, the reader is referred to the web version of this article.)

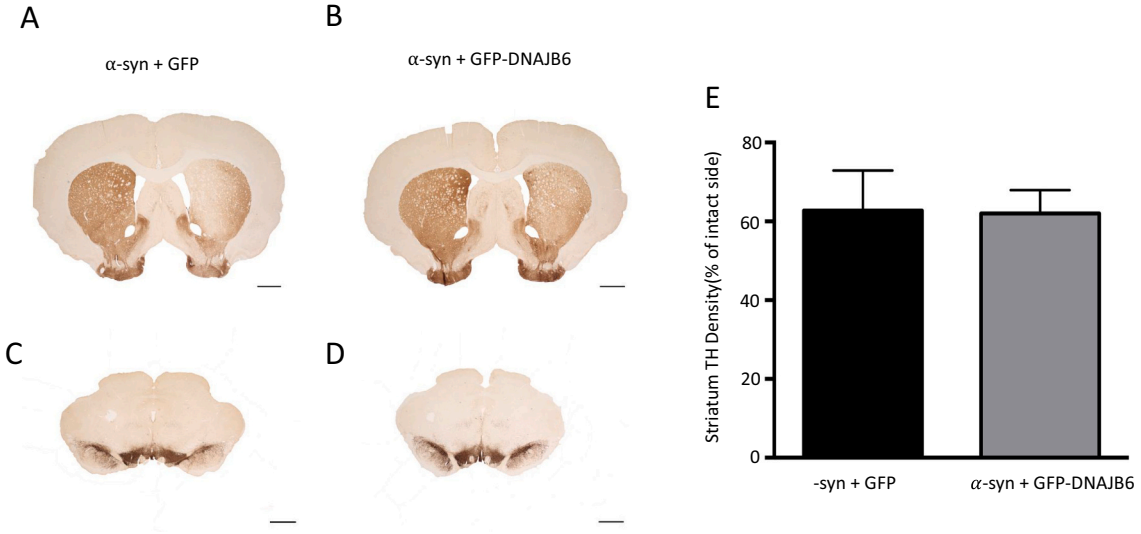

Fig. 3. Representative images of TH immunohistochemistry staining in AAV6 vira injected rats. Representative images of striatum (A) and *SN* (C) of AAV6/ human wt α-syn and AAV6/GFP injected rats. Representative images of striatum (B) and *SN* (D) of AAV6 human wt α-syn and GFP-DNAJB6 injected rats. (E) Quantification of TH+ fiber density in the striatum, expressed as a percentage of the contralateral side. $P > 0.05$ analyzed by unpaired-t-test (n:8). All data are presented as mean ± SEM. (Scale bar, 1 mm).

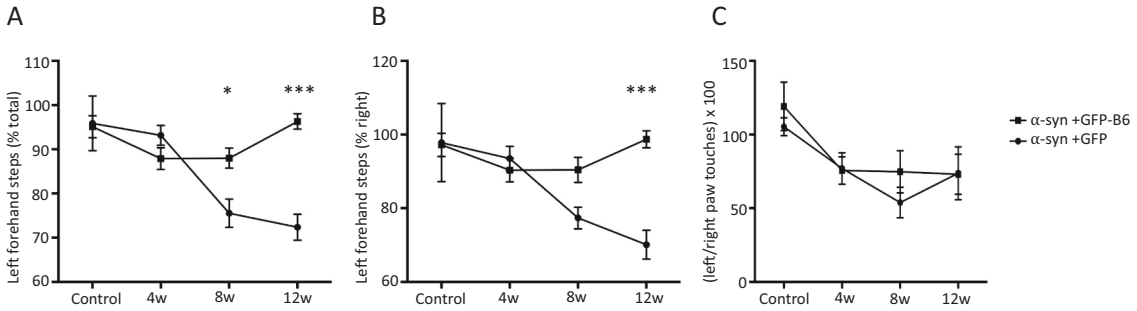

Fig. 4. DNAJB6 expression protects against behavioral deficits induced by human wt α-syn, as seen in stepping test analysis of vira injected rats. Locomotor performance was assessed using the stepping test (A and B) and cylinder test (C) at 4, 8 and 12 week time points. (A) display left forehand stepping relative percentage to total steps. (B) display left forehand steps relative to percentage of right forehand steps (C) In cylinder test, the ratio of left paw touches relative right paw touches were analyzed. All Data were analyzed by repeated measure two-way ANOVA, followed by *post hoc* Bonferroni test. All data are presented as means ± SEM. *P < 0.05, ***P < 0.001.

2010). It is therefore pivotal to find ways to decrease or prevent the α-syn aggregation. HSP70 chaperones and the DNAJ co-chaperones are proteins that have important roles in protein folding as well as re-folding or clearance of misfolded proteins (Jones et al., 2014; Hartl, 1996). There is substantial evidence that HSP70's are involved in preventing aggregated α-syn from accumulating. HSP70 may bind different α-syn species, including monomer, pre-fibrillar and fibrillar forms, and disaggregates *in vitro* (Auluck et al., 2002; Aprile et al., 2015; Gao et al., 2015; McLean et al., 2004; Nillegoda and Bukau, 2015; Rampelt et al., 2012). *In vivo*, overexpression of HSP70 reduced the amount of α-syn aggregates, in mice overexpressing α-syn (Klucken et al., 2004). In addition, our lab has shown previously that DNAJB6 is particular important in this process and that DNAJB6 works HSP70 dependently (Aprile et al., 2017; Deshayes et al., 2019; Rodriguez-Gonzalez et al., 2020).

We have previously shown that KO of DNAJB6 increases α-syn aggregation, which could be rescued by re-introduction of DNAJB6b into the cells, while we did not observe effect α-syn aggregation by KO of the DNAJB6a isoform only (Aprile et al., 2017). DNAJB6 is mainly localized in the cytosol while DNAJB6a is mainly found in the nucleus (Meng et al., 2016), which could explain why only DNAJB6b is a suppressor of α-syn aggregation. Therefore, we proceeded these studies with a focus on exploring the role of DNAJB6b, rather than DNAJB6a, in cell culture and *in vivo*. In this study, we investigated the protective role of co-chaperone DNAJB6 against α-syn aggregation and toxicity in a cell culture model as well rodent model, both based on α-syn overexpression. α-syn overexpression model has a relevant parallel for clinical cases of PD as well, as both duplication and triplication of the SNCA gene leads to a very high risk of contracting PD (Ross et al., 2008). We found that overexpression of DNAJB6b strongly suppressed aggregation of α-syn the cellular model of PD (Fig. 1). This finding supports our previous results in cellular models. Moreover, it is also in line with the results of other research labs, which suggests a general role of DNAJB6 in suppressing amyloid protein aggregation, as overexpression DNAJB6 protects from the formation of amyloid protein aggregates such as polyQ (Gillis et al., 2013; Mansson et al., 2014b; Kakkar et al., 2016) and AB42 (Mansson et al., 2014a) which are seen in Huntington's and Alzheimer's Disease, respectively. Indeed, we also found that KO of DNAJB6 in stably polyQ74exon1huntingtin (polyQ74) expressing HEK293 cells increased to polyQ74 aggregations and cell death (Rodriguez-Gonzalez et al., 2020).

The effects of DNAJB6 on amyloid protein aggregation have been investigated mostly in cellular models. Therefore, our knowledge regarding effects of DNAJB6 on amyloid protein aggregation in terms of *in vivo* studies, are still limited. However, one study has shown that DNAJB6 delays disease progression in a mouse model of HD (Kakkar et al., 2016).

DNAJB6 is highly expressed in nervous tissue and interestingly the amount of DNAJB6 is substantially increased in LB's of PD patients (Durrenberger et al., 2009). We do not yet know why DNAJB6 is found at higher levels in PD and this still remains to be explored. Our study is the first that show a protective role of DNAJ6 in an animal model of PD. We performed AAV mediated α-syn overexpression to investigated protective effects of DNAJB6 *in vivo*. This model was originally designed by Kirik et al. (Kirik et al., 2002) and mimics some of neuropathological and behavioral impairments of PD. In this work, we have revealed for the first time that overexpression of DNAJB6 protects against cell death of the dopaminergic neurons in the *SNpc* induced by α-syn overexpression (Figs. 2 and 3). We did not observe a difference in the loss of striatal TH staining between the experimental groups, but this could be because of compensatory mechanisms in the surviving TH+ neurons of the rats. However, as a consequence of the dopaminergic cell death, the rats showed impaired locomotor performance in stepping test which was progressive over a 12 week time course in the α-syn + GFP expressing rats, but not in the α-syn + GFP-DNAJB6 expressing rats (Fig. 4). We did not see any behavioral differences in the cylinder test (Fig. 4), but it is possible that in order to observe behavioral impairments in the cylinder test, then this requires a higher degree of dopaminergic cell death, than induced in this study. In line with this, Thakur et al. (Thakur et al., 2017) has shown the functional deficits in the cylinder test was not caused by either α-syn overexpression or injection of α-syn PFF's into rats, but only in the case of a combination of the two, which also resulted in a substantially higher dopaminergic cell death.

We found that the amount of total α-syn was less in the α-syn + GFP-DNAJB6 group of rats compared to the α-syn + GFP group (Fig. 3B and F). Our prior data suggest that DNAJB6 may suppress α-syn aggregation through targeting it for proteasomal degradation, which could explain these results (Deshayes et al., 2019). HSP70 family of proteins, play a role in both main protein degradation pathways, ubiquitin-proteasome system and (UPS) and autophagy-lysosome pathway (ALP) (Ciechanover and Kwon, 2017). Recently, it has proposed that while UPS is effective to degrading smaller α-syn species in young and healthy organisms, ALP is considered to be effective against larger α-syn species in aging (Ebrahimi-Fakhari et al., 2011; Emmanouilidou et al., 2010). This theory, and the observations made by Kampinga and colleagues that DNAJB6 interferes with protein aggregation in an early phase (Kakkar et al., 2016), fits in line with that the mechanism by which DNAJB6 suppress α-syn aggregation could be by targeting the smaller aggregates and delivering these to the HSP70 chaperones leading to refolding or targeting for proteosomal degradation. Overexpression of DNAJB6 did not significantly affect level of S129 phosphorylated α-syn in α-syn aggregates in neurons of *SNpc*, which was surprising to us. However, we believe that this does not exclude that that the aggregation status of α-syn is altered in the rat group overexpressing DNAJB6, compared to control group.

5. Conclusion

We have demonstrated that DNAJB6 is a strong suppressor of α-syn aggregation in cell culture as well as it protects against α-syn induced pathology in a rodent model of PD. In future, compounds that specifically target the upregulation of DNAJB6 levels, or activity of the protein, may be good future drug candidates for treatment of early stage of PD.

Ethical approval

The studies were performed in accordance with the European Union Directive (2010/63/EU) and approved by the local ethical committee for the use of laboratory animals and the Swedish Department of Agriculture (Jordbruksverket (Skåne, Sweden), permit number 8901–18).

Consent for publication

Not applicable.

Availability of data and materials

All data are used in this study are included in this article.

Funding

The authors acknowledge that the financial support from the EU Joint programme- Neurodegenerative Disease (Project name: PROTEST-70), the Royal Physiographic Society of Lund (Project Number: 40411) and Tore Nilsson Stiftelse (Project Number: 2019–00727). Sertan Arkan was supported by Stiftelsen Olle Engkvist Byggmästare.

Author contributions

Sertan Arkan contributed experimental design, execution experiments, data collection, data analysis and manuscript writing. Mårten Ljungberg execution experiments, contributed data collection and manuscript writing. Deniz Kirik contributed experimental design, data analysis and manuscript writing. Christian Hansen contributed experimental design, data collection, data analysis and manuscript writing. All authors read and approved the final manuscript.

Declaration of Competing Interest

The authors declare no competing interests.

Acknowledgement

The authors wish to thank Anneli Josefsson, Ulla Samuelsson and Björn Anzelius for their excellent technical support.

Appendix A. Supplementary data

Supplementary data to this article can be found online at https://doi.org/10.1016/j.nbd.2021.105477.

References

Aprile, F.A., Sormanni, P., Vendruscolo, M., 2015. A rational design strategy for the selective activity enhancement of a molecular chaperone toward a target substrate. Biochemistry. 54 (32), 5103–5112.
Aprile, F.A., Kallstig, E., Limorenko, G., Vendruscolo, M., Ron, D., Hansen, C., 2017. The molecular chaperones DNAJB6 and Hsp70 cooperate to suppress alpha-synuclein aggregation. Sci. Rep. 7 (1), 9039.
Auluck, P.K., Chan, H.Y., Trojanowski, J.Q., Lee, V.M., Bonini, N.M., 2002. Chaperone suppression of alpha-synuclein toxicity in a Drosophila model for Parkinson's disease. Science. 295 (5556), 865–868.
Balch, W.E., Morimoto, R.I., Dillin, A., Kelly, J.W., 2008. Adapting proteostasis for disease intervention. Science. 319 (5865), 916–919.
Bonini, N.M., Giasson, B.I., 2005. Snaring the function of alpha-synuclein. Cell. 123 (3), 359–361.
Burre, J., Sharma, M., Tsetsenis, T., Buchman, V., Etherton, M.R., Sudhof, T.C., 2010. Alpha-synuclein promotes SNARE-complex assembly in vivo and in vitro. Science. 329 (5999), 1663–1667.
Ciechanover, A., Kwon, Y.T., 2017. Protein quality control by molecular chaperones in Neurodegeneration. Front. Neurosci. 11, 185.
Cuervo, A.M., Stefanis, L., Fredenburg, R., Lansbury, P.T., Sulzer, D., 2004. Impaired degradation of mutant alpha-synuclein by chaperone-mediated autophagy. Science. 305 (5688), 1292–1295.
De Mattos, E.P., Wentink, A., Nussbaum-Krammer, C., Hansen, C., Bergink, S., Melki, R., et al., 2020. Protein quality control pathways at the crossroad of Synucleinopathies. J. Parkinsons Dis. 10 (2), 369–382.
Deshayes, N., Arkan, S., Hansen, C., 2019. The molecular chaperone DNAJB6, but Not DNAJB1, suppresses the seeded aggregation of alpha-synuclein in cells. Int. J. Mol. Sci. 20 (18).
Durrenberger, P.F., Filiou, M.D., Moran, L.B., Michael, G.J., Novoselov, S., Cheetham, M. E., et al., 2009. DnaJB6 is present in the core of Lewy bodies and is highly up-regulated in parkinsonian astrocytes. J. Neurosci. Res. 87 (1), 238–245.
Ebrahimi-Fakhari, D., Cantuti-Castelvetri, I., Fan, Z., Rockenstein, E., Masliah, E., Hyman, B.T., et al., 2011. Distinct roles in vivo for the ubiquitin-proteasome system and the autophagy-lysosomal pathway in the degradation of alpha-synuclein. J. Neurosci. 31 (41), 14508–14520.
Emmanouilidou, E., Stefanis, L., Vekrellis, K., 2010. Cell-produced alpha-synuclein oligomers are targeted to, and impair, the 26S proteasome. Neurobiol. Aging 31 (6), 953–968.
Fujiwara, H., Hasegawa, M., Dohmae, N., Kawashima, A., Masliah, E., Goldberg, M.S., et al., 2002. Alpha-Synuclein is phosphorylated in synucleinopathy lesions. Nat. Cell Biol. 4 (2), 160–164.
Gao, X., Carroni, M., Nussbaum-Krammer, C., Mogk, A., Nillegoda, N.B., Szlachcic, A., et al., 2015. Human Hsp70 Disaggregase reverses Parkinson's-linked alpha-Synuclein amyloid fibrils. Mol. Cell 59 (5), 781–793.
Gillis, J., Schipper-Krom, S., Juenemann, K., Gruber, A., Coolen, S., van den Nieuwendijk, R., et al., 2013. The DNAJB6 and DNAJB8 protein chaperones prevent intracellular aggregation of polyglutamine peptides. J. Biol. Chem. 288 (24), 17225–17237.
Goedert, M., Spillantini, M.G., Del Tredici, K., Braak, H., 2013. 100 years of Lewy pathology. Nat. Rev. Neurol. 9 (1), 13–24.
Hansen, C., Li, J.Y., 2012. Beyond alpha-synuclein transfer: pathology propagation in Parkinson's disease. Trends Mol. Med. 18 (5), 248–255.
Hartl, F.U., 1996. Molecular chaperones in cellular protein folding. Nature. 381 (6583), 571–579.
Hartl, F.U., Bracher, A., Hayer-Hartl, M., 2011. Molecular chaperones in protein folding and proteostasis. Nature. 475 (7356), 324–332.
Holmes, B.B., Furman, J.L., Mahan, T.E., Yamasaki, T.R., Mirbaha, H., Eades, W.C., et al., 2014. Proteopathic tau seeding predicts tauopathy in vivo. Proc. Natl. Acad. Sci. U. S. A. 111 (41), E4376–E4385.
Jones, D.R., Moussaud, S., McLean, P., 2014. Targeting heat shock proteins to modulate alpha-synuclein toxicity. Ther. Adv. Neurol. Disord. 7 (1), 33–51.
Kakkar, V., Mansson, C., de Mattos, E.P., Bergink, S., van der Zwaag, M., van Waarde, M., et al., 2016. The S/T-rich motif in the DNAJB6 chaperone delays Polyglutamine aggregation and the onset of disease in a mouse model. Mol. Cell 62 (2), 272–283.
Kirik, D., Rosenblad, C., Bjorklund, A., Mandel, R.J., 2000. Long-term rAAV-mediated gene transfer of GDNF in the rat Parkinson's model: intrastriatal but not intranigral transduction promotes functional regeneration in the lesioned nigrostriatal system. J. Neurosci. 20 (12), 4686–4700.
Kirik, D., Rosenblad, C., Burger, C., Lundberg, C., Johansen, T.E., Muzyczka, N., et al., 2002. Parkinson-like neurodegeneration induced by targeted overexpression of alpha-synuclein in the nigrostriatal system. J. Neurosci. 22 (7), 2780–2791.
Klucken, J., Shin, Y., Masliah, E., Hyman, B.T., McLean, P.J., 2004. Hsp70 reduces alpha-Synuclein aggregation and toxicity. J. Biol. Chem. 279 (24), 25497–25502.
Landeck, N., Hall, H., Ardah, M.T., Majbour, N.K., El-Agnaf, O.M., Halliday, G., et al., 2016. A novel multiplex assay for simultaneous quantification of total and S129 phosphorylated human alpha-synuclein. Mol. Neurodegener. 11 (1), 61.
Logan, T., Bendor, J., Toupin, C., Thorn, K., Edwards, R.H., 2017. Alpha-Synuclein promotes dilation of the exocytotic fusion pore. Nat. Neurosci. 20 (5), 681–689.
Mansson, C., Arosio, P., Hussein, R., Kampinga, H.H., Hashem, R.M., Boelens, W.C., et al., 2014a. Interaction of the molecular chaperone DNAJB6 with growing amyloid-beta 42 (Abeta42) aggregates leads to sub-stoichiometric inhibition of amyloid formation. J. Biol. Chem. 289 (45), 31066–31076.
Mansson, C., Kakkar, V., Monsellier, E., Sourigues, Y., Harmark, J., Kampinga, H.H., et al., 2014b. DNAJB6 is a peptide-binding chaperone which can suppress amyloid fibrillation of polyglutamine peptides at substoichiometric molar ratios. Cell Stress Chaperones 19 (2), 227–239.
McLean, P.J., Klucken, J., Shin, Y., Hyman, B.T., 2004. Geldanamycin induces Hsp70 and prevents alpha-synuclein aggregation and toxicity in vitro. Biochem. Biophys. Res. Commun. 321 (3), 665–669.
Meng, E., Shevde, L.A., Samant, R.S., 2016. Emerging roles and underlying molecular mechanisms of DNAJB6 in cancer. Oncotarget. 7 (33), 53984–53996.
Nillegoda, N.B., Bukau, B., 2015. Metazoan Hsp70-based protein disaggregases: emergence and mechanisms. Front. Mol. Biosci. 2, 57.
Paxinos, G., Watson, C., 2006. The Rat Brain in Stereotaxic Coordinates. Academic Press.
Qiu, X.B., Shao, Y.M., Miao, S., Wang, L., 2006. The diversity of the DnaJ/Hsp40 family, the crucial partners for Hsp70 chaperones. Cell. Mol. Life Sci. 63 (22), 2560–2570.

Rampelt, H., Kirstein-Miles, J., Nillegoda, N.B., Chi, K., Scholz, S.R., Morimoto, R.I., et al., 2012. Metazoan Hsp70 machines use Hsp110 to power protein disaggregation. EMBO J. 31 (21), 4221–4235.
Rodriguez-Gonzalez, C., Lin, S., Arkan, S., Hansen, C., 2020. Co-chaperones DNAJA1 and DNAJB6 are critical for regulation of polyglutamine aggregation. Sci. Rep. 10 (1), 8130.
Ross, O.A., Braithwaite, A.T., Skipper, L.M., Kachergus, J., Hulihan, M.M., Middleton, F. A., et al., 2008. Genomic investigation of alpha-synuclein multiplication and parkinsonism. Ann. Neurol. 63 (6), 743–750.
Spillantini, M.G., Schmidt, M.L., Lee, V.M., Trojanowski, J.Q., Jakes, R., Goedert, M., 1997. Alpha-synuclein in Lewy bodies. Nature. 388 (6645), 839–840.
Thakur, P., Breger, L.S., Lundblad, M., Wan, O.W., Mattsson, B., Luk, K.C., et al., 2017. Modeling Parkinson's disease pathology by combination of fibril seeds and alpha-synuclein overexpression in the rat brain. Proc. Natl. Acad. Sci. U. S. A. 114 (39). E8284-E93.
Ulusoy, A., Bjorklund, T., Buck, K., Kirik, D., 2012. Dysregulated dopamine storage increases the vulnerability to alpha-synuclein in nigral neurons. Neurobiol. Dis. 47 (3), 367–377.
Vekrellis, K., Xilouri, M., Emmanouilidou, E., Rideout, H.J., Stefanis, L., 2011. Pathological roles of alpha-synuclein in neurological disorders. Lancet Neurol. 10 (11), 1015–1025.
Venda, L.L., Cragg, S.J., Buchman, V.L., Wade-Martins, R., 2010. Alpha-Synuclein and dopamine at the crossroads of Parkinson's disease. Trends Neurosci. 33 (12), 559–568.
Waxman, E.A., Giasson, B.I., 2009. Molecular mechanisms of alpha-synuclein neurodegeneration. Biochim. Biophys. Acta 1792 (7), 616–624.